JOURNAL OF MATERIALS SCIENCE 21 (1986) 429–434

The effect of DO_3 ordering on the parent $\rightleftarrows$ martensitic transformation in the CuZnAl shape-memory alloy

J. DUTKIEWICZ, J. MORGIEL
Institute for Metal Research of the Polish Academy of Sciences, Kraków, ul. Reymonta 25, Poland

The character of DO_3 ordering resulting from different quenching rates and its effect on the characteristic martensitic transformation temperatures and shape-memory effect in the Cu–21.5 at % Zn–12.5 at % Al alloy has been analysed. In room temperature water-quenched samples with a cooling rate $\sim 1000^\circ C\,sec^{-1}$ showing B2 long-range order and DO_3 short-range order, a significant stabilization of martensite in the reverse transformation was observed. This stabilization was eliminated in the air-cooled samples with a cooling rate $\sim 20^\circ C\,sec^{-1}$ showing DO_3 long-range order. Mechanical tests revealed a more complete shape recovery in the air-cooled samples, when compared to room temperature water-quenched ones.

1. Introduction

The shape-memory effect occurs only in ordered alloys undergoing martensitic transformation [1, 2]. In binary copper alloys the metastable low temperature β_1 phase possesses either a B2(CuZn) or $DO_3(Cu_3Al)$ superlattice [3, 4]. The first of these exists in all ternary CuZnAl alloys within the composition range where $e/a \sim 3/2$, but there are still some doubts about the range of appearance of the DO_3 ordering.

Melton and Mercier [5] stated that in these alloys the DO_3 ordering begins above 14 at % Al, which contradicts other results as summarized by Dunne and Kennon [6], who found that DO_3 can be introduced into material by quenching into boiling water. This dependence upon quenching rates corroborates the fact that in the rapidly solidified CuZn–16 at % Al alloys only B2 order is formed [7].

In the present study, samples have been quenched at different rates in order to explain the effect of quenching rate on the formation of DO_3 superstructure and the reversible martensitic transformation.

2. Experimental procedure

The CuZnAl alloy containing 21.5 at % Zn and 12.5 at % Al was chosen for this investigation since, after quenching into room temperature water, it should possess only B2 type ordering [5]. The alloy was prepared from high purity materials (impurities less than 0.01 wt %). The ingot, after casting, was homogenized at 650° C for 4 h in an argon atmosphere, then hot rolled to ~0.25 mm sheet. The samples were solution-treated in the β-phase field at 850° C, then quenched into various cooling media: room-temperature water (cooling rate $\sim 1000^\circ C\,sec^{-1}$), 100° C water ($\sim 500^\circ C\,sec^{-1}$) and air ($\sim 20^\circ C\,sec^{-1}$). Mechanical tests and electrical conductivity experiments were performed immediately after quenching to avoid any low-temperature ageing.

A Philips EM–301 transmission electron microscope (TEM) fitted with a goniometer stage and a Rigaku Denki diffractometer were used to determine the crystal structure of the samples. Thin foils for TEM were prepared by jet electropolishing in a solution of H_3PO_4 saturated with CrO_3 diluted 1 : 1 with H_3PO_4 at room temperature and a potential of 10 V. Domain size was measured directly from the micrographs using the mean intercept distance [8]. The transformation behaviour was followed using electrical conductivity measurements. The heating or cooling rate was approximately 2.5 deg min^{-1}. Stress–strain curves illustrating the shape-memory effect were obtained with an Instron testing machine fitted with a low-temperature attachment.

3. Results

X-ray and electron diffraction indicated the presence of β_1 parent and β_1' martensite phases in samples quenched to room temperature at different rates. No traces of α or bainitic phases were detected. A typical example of the finely striated martensitic microstructure can be seen in the sample quenched into water at room temperature (Fig. 1a). The corresponding electron diffraction pattern (Fig. 1b) shows the $[0\,1\,0]\beta_1'$ zone axis orientation with $(1, 0, 4 \pm 6n)$ rows of spots denoting the existence of 18R superstructure.

Figs. 2 to 4 are taken from samples quenched at successively slower quenching rates, and show sets of electron diffraction patterns with exactly or close to [0 1 1] orientation of the parent β_1 phase, and two corresponding dark-field micrographs showing the B2 and DO_3 antiphase domains, respectively. All diffraction patterns show superlattice spots characteristic for

0022–2461/86 $03.00 + .12

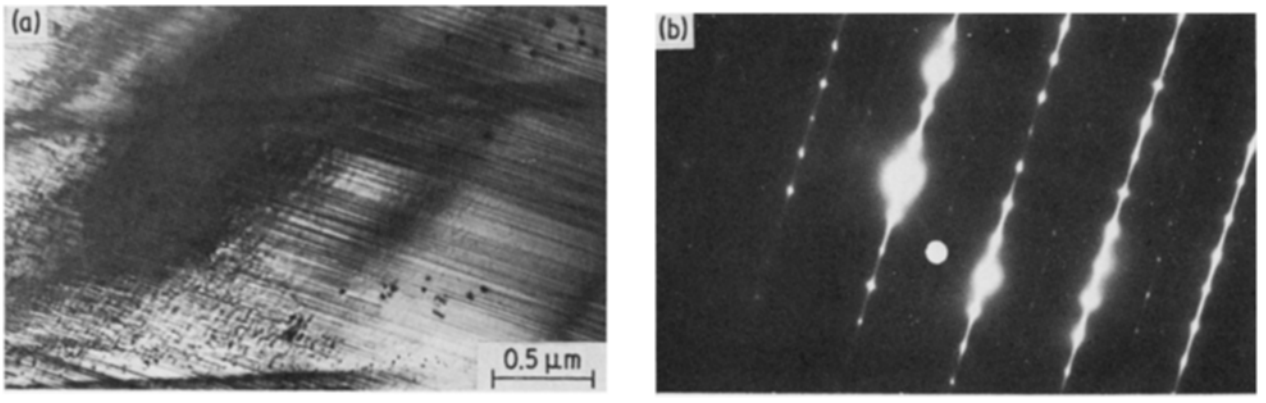

Figure 1 Room temperature water-quenched sample: (a) bright-field transmission electron micrograph; (b) electron diffraction pattern.

both B2 order as $\{1\,0\,0\}$, $\{1\,1\,1\}$ in bcc notation, and for DO_3 as $\{\frac{1}{2}\,\frac{1}{2}\,\frac{1}{2}\}$, $\{\frac{3}{2}\,\frac{1}{2}\,\frac{1}{2}\}$ bcc. However, because of small deviation from the exact [0 1 1] zone axis orientation in Figs. 2b and 4b, their absolute intensity cannot be compared. The additional spots, lying inside diffuse streaks, result from the presence of the pre-martensitic Sato structure, and can be indexed accordingly to Murakami *et al.* [9].

The B2 antiphase domains are shown in Figs. 2b to 4b. The mean domain size grows approximately from 0.12 μm (Fig. 2b) to 0.36 μm (Fig. 3b) and to more than 3.6 μm (Fig. 4b). The dark-field micrographs presented in Figs. 2c to 4c, taken using $(1\,1\,1)\beta_1$ reflections, show DO_3 domains. Although the DO_3 superlattice spots are clearly visible in all diffraction patterns, only in one sample, which has undergone the slowest quench, are the DO_3 domains of a size of 0.06 μm which can be easily measured (Fig. 4c). This micrograph shows a trace of the B2 antiphase domain boundary as well. It can be seen there that DO_3 domain boundaries match the B2 one, as indicated by arrows in the enlargement shown in Fig. 5. In water-quenched samples the domains can be seen as dots with diffuse boundaries. In the room temperature water-quenched sample domains are barely visible, which means that only short-range order (SRO) has been formed. After the first thermal cycle the room temperature water-quenched sample shows an increase in DO_3 superlattice spots and domain contrast (Fig. 6), and this was confirmed in other micrographs.

Fig. 7 presents the electrical resistivity against temperature curves with marked M_s, M_f and A_s, A_f temperatures for samples quenched under different conditions. The first cycles are drawn with a dashed line and the transformation temperatures are given a superscript 1. Arrows indicate the direction of temperature change in a given cycle. It can be seen that loops describing the cooling/heating cycle shrink rapidly with lowering of the quenching rate, as the second loops (full line, characteristic temperatures marked with superscript 2) remain nearly unaffected. It is easier to follow this change by observing variations in the phase transformation temperatures given in Table I.

The difference between the first and subsequent martensitic transformation temperatures shows only for the room temperature water-quenched sample (Fig. 7a). The reverse transformation is much more affected by the quenching rate (Fig. 7b). The largest

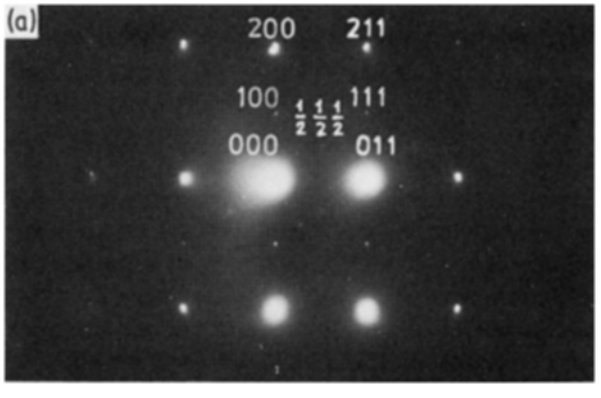

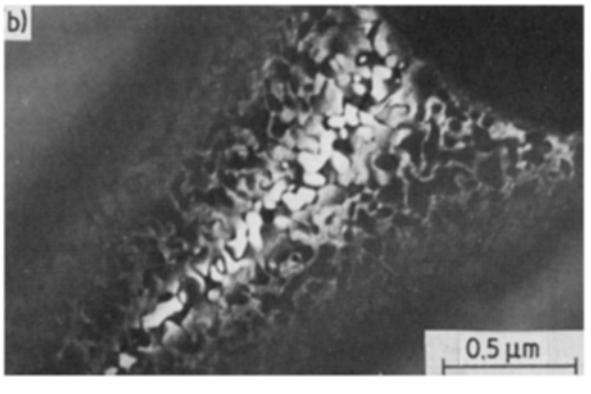

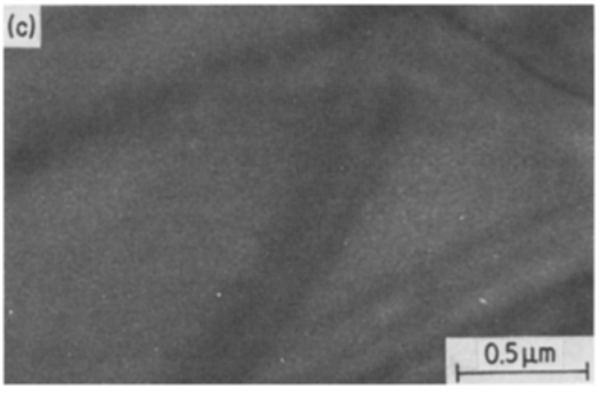

Figure 2 Room temperature water-quenched sample: (a) electron diffraction pattern; (b) dark-field image taken using (1 0 0) superlattice spot; (c) dark-field image taken using $(\frac{1}{2}\,\frac{1}{2}\,\frac{1}{2})$ superlattice spot.

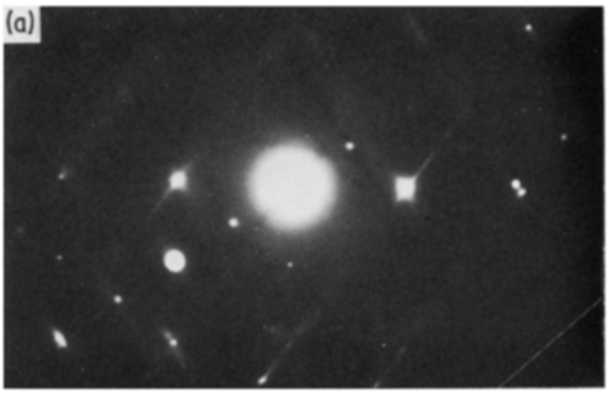

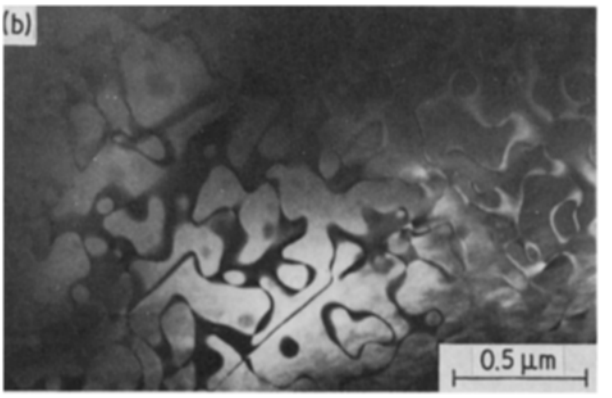

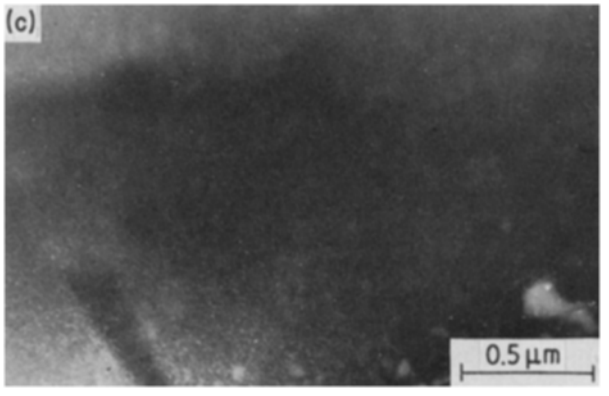

Figure 3 100° C water-quenched sample: (a) electron diffraction pattern; (b) dark-field image taken using (1 1 1) superlattice spot; (c) dark-field image taken using $(\frac{1}{2}\frac{1}{2}\frac{1}{2})$ superlattice spot.

change between A_f^1 and A_f^2 shows also in the above-mentioned sample, as the end of its first reverse process is delayed by 40° C. The A_s^2 temperature is about 5° C lower then A_s^1 in each sample, and they both move up the temperature scale with lowering quenching rates.

Fig. 8 shows stress–strain curves illustrating the shape memory effect after a temperature change from − 196° C (tension test temperature) to + 100° C (unloading temperature). It can be seen that the hysteresis loop of the first cycle of the sample quenched in room temperature water is broader then that of the air-cooled sample. The second cycle provides tighter hysteresis in both samples and complete shape recovery.

4. Discussion

In samples quenched into room temperature water, weak DO_3 superlattice spots were found in the β_1 parent and consequently 18R in the β_1' martensite diffraction pattern. The corresponding DO_3 antiphase domains are very small, a few nanometres in diameter. Rapacioli and Ahlers [10] examined ordering in an alloy with an even lower aluminium addition (10.4 at % Al) and also found DO_3 domains in a dot form, characteristic of SRO [11]. Both the above results disagree with the explanation by Melton and Mercier [5], that the minimum in the $\sigma_{0.2}$ (0.2 pct proof stress) at 14 at % Al can be connected with a change in order type from B2/9R to DO_3/18R. In rapidly solidified alloys only B2/9R order is formed unless the aluminium contents are above 16 at % [7]. The results are consistent with the fact that the B2 → DO_3 transition is of the first order and, as such, can be suppressed by rapid quenching [6]. Thereafter, in these alloys quenched into room temperature water DO_3 ordering is of SRO type and starts from below 10 at % Al ($e/a = 3/2$).

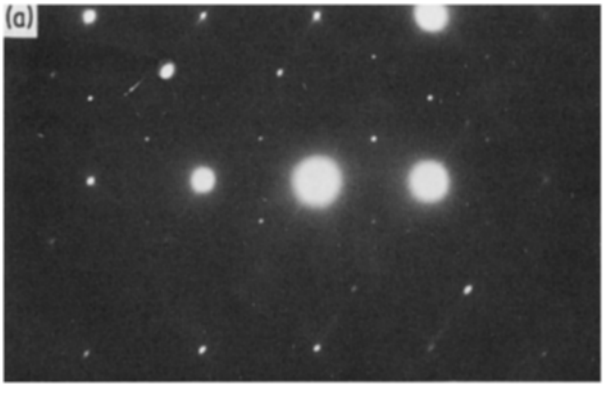

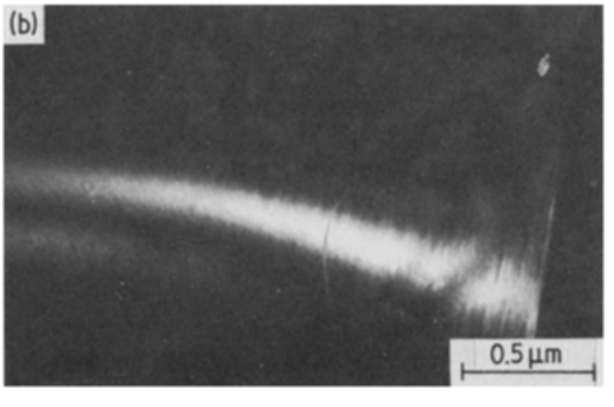

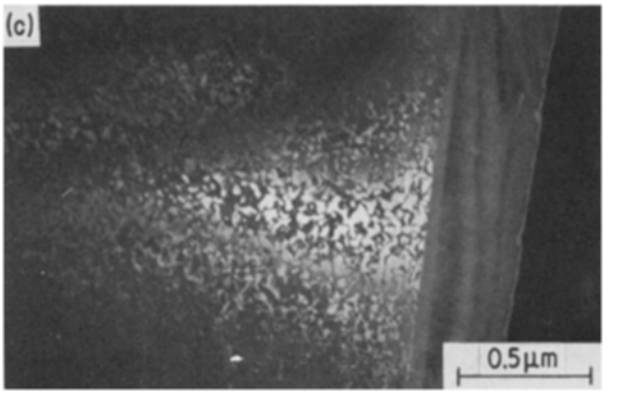

Figure 4 Air-cooled sample: (a) electron diffraction pattern; (b) dark-field image taken using (1 0 0) superlattice spot; (c) dark-field image taken using $(\frac{3}{2}\frac{1}{2}\frac{1}{2})$ superlattice spot.

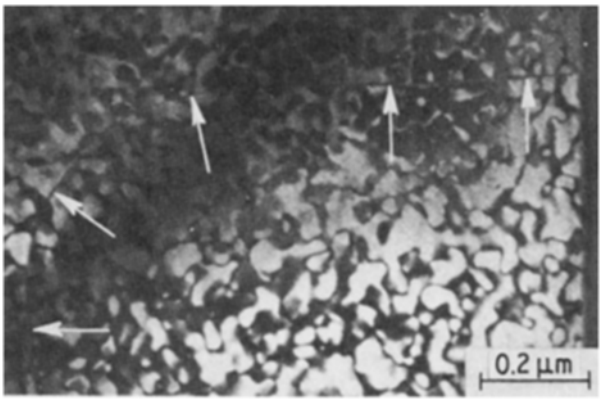

Figure 5 Enlarged portion of Fig. 4c showing trace of B2 domain boundary (marked with arrows) matching DO_3 boundaries.

As with previous results [7, 12], it is observed in the present work that there is an upward shift of the martensitic start temperature M_s with cycling. The explanation of these changes by increased ordering [7] seems to be valid, as in air-cooled samples this shift is significantly reduced and the subsequent martensitic transformations do not differ with regard to M_s and M_f temperatures (Fig. 7 and Table I). Another result of the resistivity against temperature measurements is stabilization of martensite in the first heating cycle in the room temperature water-quenched sample, resulting in an increase of A_f temperature. Similar results have been reported [6, 13–16, 17] but various explanations have been proposed, namely:

(a) introduction of internal stresses, due primarily to rapid quenching, promoting formation of the α (3R) martensite [13];

(b) reordering of non-transformed β_1 phase from B2 to DO_3 and formation of "uncoupled" interfaces with 9R martensite [6]; and

(c) migration of vacancies to martensite plates boundaries where they are pinned on [14, 15].

TABLE I Transition temperature

Transition	Temperature (° C)		
	Room temperature water-quenched	100° C water-quenched	Air-cooled
M_s^1	~20	~30	~30
M_s^2	30	30	30
A_s^1	5	15	20
A_s^2	0	10	15
M_f^1	−20	−5	−5
M_f^2	−15	−5	−5
A_f^1	70	50	40
A_f^2	35	40	35

The first of these, (a), has an insignificant influence in the alloy investigated, since no dependence of martensite structure on cooling rate was observed. The formation of "uncoupled" interfaces, (b), looks quite possible, as the lower quenching rate (and thereafter higher ordering, Fig. 8) did not cause a stabilization of martensite. However, this model ought to be slightly modified as the alloy investigated in this work possesses DO_3 SRO already after quenching into room temperature water, and the volume of non-transformed β_1 phase was very small. It is proposed that "uncoupled" interfaces develop between parts which first re-transformed to the parent phase and that of martensite. This difference lies in the degree, not in the type of order. Such a difference in ordering kinetics is caused by much faster diffusion in β_1 than β_1' [18]. The proposed modification, introducing a constant inflow of obstacles in the form of new "uncoupled" interfaces during reverse martensitic transformation, fits well the observation that A_s^1 and A_s^2 are nearly the same and only A_f^1 is shifted well above A_f^2 in the temperature scale. It means that reverse transformation is only slowed down but not retarded as a whole. Such behaviour can also be seen on the resistivity against temperature curves measured

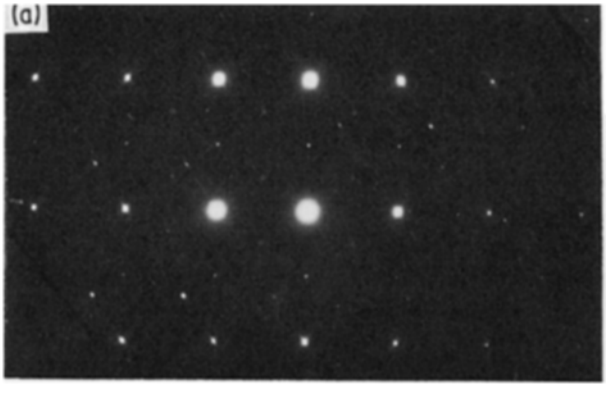

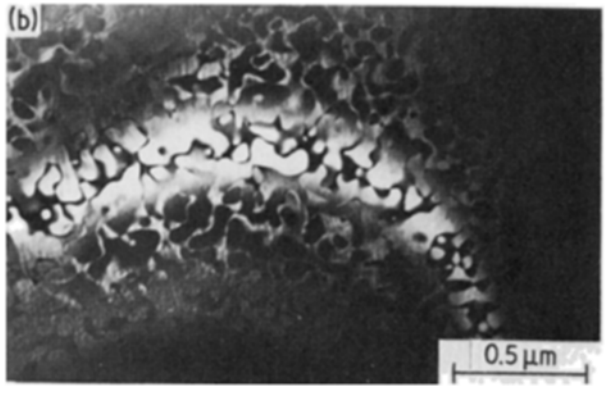

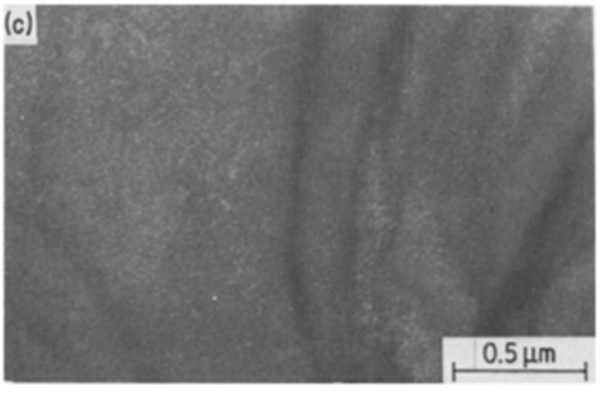

Figure 6 Room temperature water-quenched sample after one transformation cycle: (a) electron diffraction pattern; (b) dark-field image taken using (1 0 0) superlattice spot; (c) dark-field image taken using $(\frac{1}{2}\frac{1}{2}\frac{1}{2})$ superlattice spot.

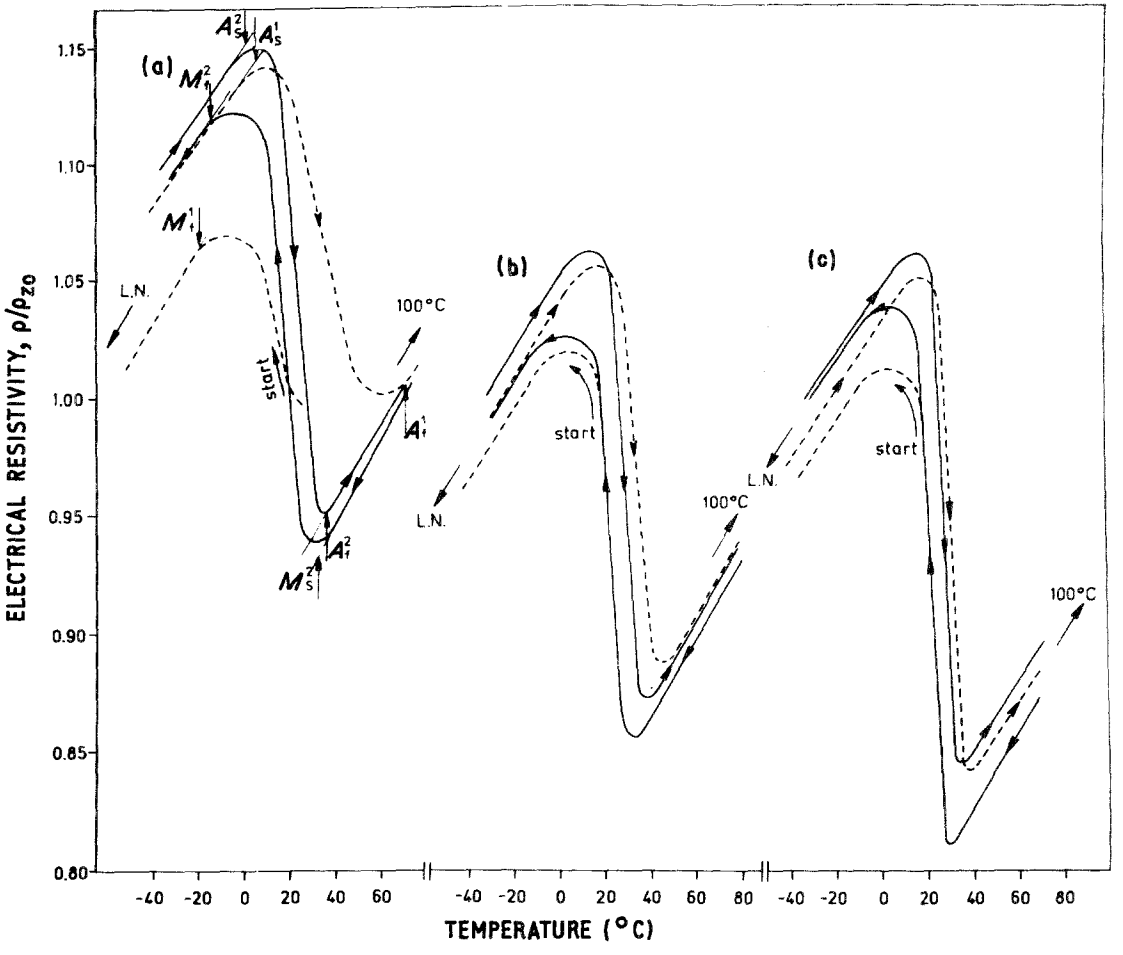

Figure 7 Electrical resistivity against temperature curves taken from (a) room temperature water-quenched sample, (b) 100° C water-quenched sample, and (c) air-cooled sample. Dashed line, first cycle; solid line, second cycle. (L.N. is liquid nitrogen).

by Janssen *et al.* [14], but contradicts that presented by Delaey *et al.* [13]. The last supposition, (c), connecting stabilization of martensite with vacancy migration is difficult to distinguish from ordering, as these processes overlap and are probably acting together.

The mechanical behaviour of samples in the martensitic condition also seem to be affected by increased ordering. The air-cooled sample shows a smaller permanent plastic deformation, and hence better shape recovery than the room temperature water-quenched one, as was previously observed on samples tested by bending [17].

5. Conclusions

1. The character of DO_3 ordering in CuZnAl alloys depends on the quenching rate; in room temperature water-quenched samples (cooling rate $\sim 1000°\,C\,sec^{-1}$) it is of short-range order type, and in air-cooled samples (cooling rate $20°\,C\,sec^{-1}$) of long-range order type. In the same samples the size of the B2 long-range order domains increases with decreasing quenching rate.

2. The stabilization of martensite in the reverse transformation, observed only in the first cycle, can be eliminated by a lower quenching rate introducing DO_3 long-range order.

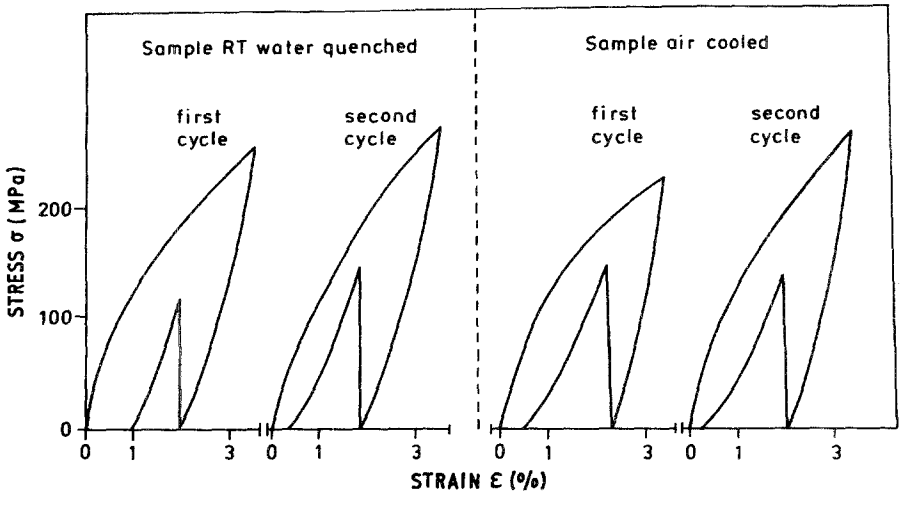

Figure 8 Stress–strain curves of (a) room temperature water-quenched, and (b) air-cooled samples.

3. The air-cooled samples show better shape recovery, when compared with the room temperature water-quenched ones.

References

1. C. M. WAYMAN and K. SHIMIZU, *Met. Sci. J.* **6** (1972) 175.
2. K. SHIMIZU, *Mem. Inst. Sci. Ind. Res. Osaka Univ.* **34** (1977) 9.
3. H. WARLIMONT and L. DELAEY, *Prog. Mater. Sci.* **18** (1974) 6.
4. Z. NISHIYAMA, "Martensitio Transformation" (Academic Press, New York, 1978) p. 74.
5. K. N. MELTON and O. MERCIER, *Metall. Trans.* **10A** (1979) 875.
6. D. P. DUNNE and N. F. KENNON, *Scripta Metall.* **16** (1982) 729.
7. J. PERKINS, *Metall. Trans.* **13A** (1982) 1367.
8. D. G. MORRIS, G. T. BROWN, R. C. PILLER and R. E. SMALLMAN, *Acta Metall.* **24** (1978) 21.
9. Y. MURAKAMI, L. DELAEY and G. SEEMSTER-DULLENKOPF, *Trans. Jpn. Insts. Met.* **19** (1978) 317.
10. R. RAPACIOLI and M. AHLERS, *Scripta Metall.* **11** (1977) 1147.
11. S. K. DAS and G. THOMAS, Proceedings of International Symposium on Order–Disorder Transformation, Tubingen, 1973 (Springer-Verlag, Berlin, 1974) p. 332.
12. J. PERKINS, *J. Phys.* **43** (1982) C4–697.
13. L. DELAEY, J. VAN HUMBEECK, M. CHANDRASEKARAN, J. JANSSEN, M. ANDRADE and N. MWAMBA, *Met. Forum* **4** (1981) 164.
14. J. JANSSEN, J. VAN HUMBEECK, M. CHANDRASEKARAN, M. MWAMBA and L. DELAEY, *J. Phys.* **43** (1982) C4–715.
15. Z. BOJARSKI, H. MORAWIEC, J. ILLCZUK, T. PANEK and M. AUGUSTNIAK, Proceedings of XI Metallography Conference, Częstochowa, 1983 (SITPH, Katowice, 1983) p. 245.
16. J. DUTKIEWICZ, J. MORGIEL and W. BALIGA, Proceedings of XI Metallography Conference, Częstochowa 1983 (SITPH, Katowice, 1983) p. 239.
17. G. Y. YAROSLAVSKI, S. Y. KONDRAT'YEV, Y. N. KOVALEV, R. J. MUSIENKO and B. S. CHAIKOWSKI, *Fiz. Met. Metall.* **54** (1982) 597.
18. L. DELAEY, A. DERUYTTERE, E. ARNOUDT and J. R. ROOS, INCRA Report 78 (Katholieke University Leuven, 1978) p. 51.

Received 5 July 1984
and accepted 28 February 1985